

Excitonic Mott transition in type-II quantum dots

Bhavtosh Bansal,^{1,*} M. Hayne,^{1,2} M. Geller,³ D. Bimberg,³ and V. V. Moshchalkov¹

¹INPAC-Institute for Nanoscale Physics and Chemistry, Pulsed Fields Group, Katholieke Universiteit Leuven, Celestijnenlaan 200D, Leuven B-3001, Belgium

²Department of Physics, Lancaster University, Lancaster LA1 4YB, United Kingdom

³Institut für Festkörperphysik, PN 5-2, Hardenbergstrasse 36, 10623 Berlin, Germany

(Received 4 April 2008; revised manuscript received 20 May 2008; published 13 June 2008)

Photoluminescence spectra measured on a type-II GaSb/GaAs quantum dot ensemble at high excitation power indicate a Mott transition from the low density state comprising of spatially indirect excitons to a high density electron-plasma state. Under the influence of a very high magnetic field, the electron-plasma that is formed at high excitation powers is transformed into magneto-excitons.

DOI: 10.1103/PhysRevB.77.241304

PACS number(s): 78.67.Hc, 71.35.Lk, 71.35.Ji

Photoexcited carriers in a semiconductor are a model system where we have the means to both controllably generate and, through the recombination luminescence, probe the energy levels and statistics of the exciton population. At low excitation power, Wannier excitons can be treated as independent, similar to a gas of noninteracting hydrogenic atoms. A larger density of such entities can lead to the formation of molecular, liquid, metallic, or superfluid phases.^{1,2} The low and high density regimes are also separated by a Mott transition between the “insulating” excitonic state of bound electron-hole pairs and the plasma state.^{3,4}

In this Rapid Communication we report photoluminescence (PL) measurements of a type-II self-assembled quantum dot (QD) ensemble. Due to the staggered band alignment at the GaSb-GaAs interface,⁵⁻⁷ the GaSb QDs contained within the GaAs matrix confine the holes, but act as antidots for the electrons (Fig. 1). Under nonresonant optical excitation, the electron-hole pairs generated are spatially separated, with the electrons being loosely bound to the charge of the holes within the QDs.^{6,7} The charge distribution of the excluded electrons is self-consistently determined such that it corresponds to the minimum energy configuration,⁸ possibly with interesting topological consequences.^{8,9} These excitons have no center of mass degree of freedom and the average charge of the QDs can be tuned by the strength of the optical excitation.^{7,10,11} They do not form excitonic “molecules;” the biexcitons are rather similar to new “elements” with different “nuclear” charge.^{7,10} The upper bound of the exciton density is determined by the spatial density of the randomly positioned QDs. Studying the PL spectra from GaSb QDs at different excitation powers and in high mag-

netic fields, we have encountered two Mott transitions. The first is a transition from the noninteracting excitonic gas state to a plasma state as a result of increased optical excitation, while the second is a transition back to an (optically inactive) exciton state as a result of the application of a very large magnetic field (≤ 45 T). The former is typical of excitonic systems, while the latter is characteristic of impurity bands. Thus we have probed the entire Mott-transition phase diagram in a system that displays properties associated with both excitons and donor impurities.

Sample growth (by metal-organic vapor phase epitaxy) and characterization is described in Ref. 5. The sample measured in this study corresponds to a growth interruption of 2 seconds and a QD density of about $3 \times 10^{10} \text{ cm}^{-2}$. While transmission electron microscope images⁵ seemed to suggest

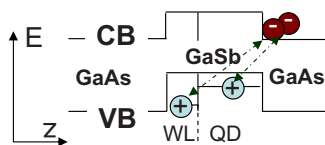


FIG. 1. (Color online) Simplified band diagram showing spatially indirect excitons with electrons in the GaAs matrix and holes in the GaSb valence band of the WL and QD. The z axis denotes the growth direction and the QDs are distributed in the xy plane. The band diagram from an eight-band $\mathbf{k} \cdot \mathbf{p}$ calculation can be found in Ref. 7

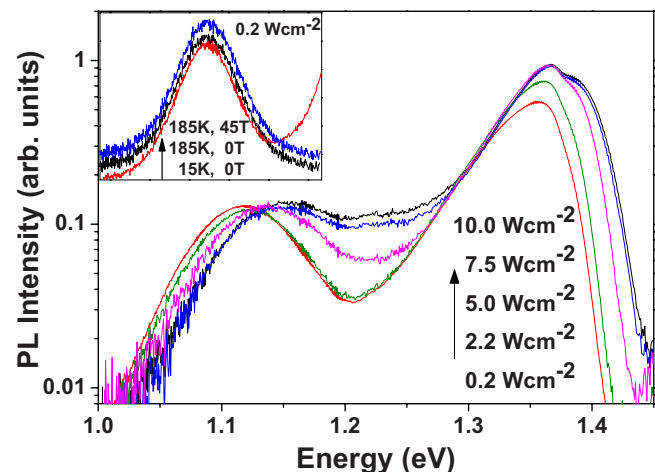


FIG. 2. (Color online) The zero-field PL spectra at different excitation powers measured at 15 K. The emission around 1.1 eV is from QDs and the higher energy peak is due to the WL. The QD spectra considerably broaden at higher excitation powers, indicating the loss of excitonic resonance. The asymmetry and shoulder in the WL peak is due to the sharp cutoff in the detector response at ~ 1.38 eV. (Inset) A comparison of line shapes for the 0.2 W cm^{-2} spectra (linear scale, offset on both x and y axes and normalized), measured at 15 K ($B=0$ T) and 185 K ($B=0$ T, 45 T), show that at this low power the emission linewidth and the (Gaussian) spectral shape are completely determined by the inhomogeneous broadening and are independent of magnetic field and temperature.

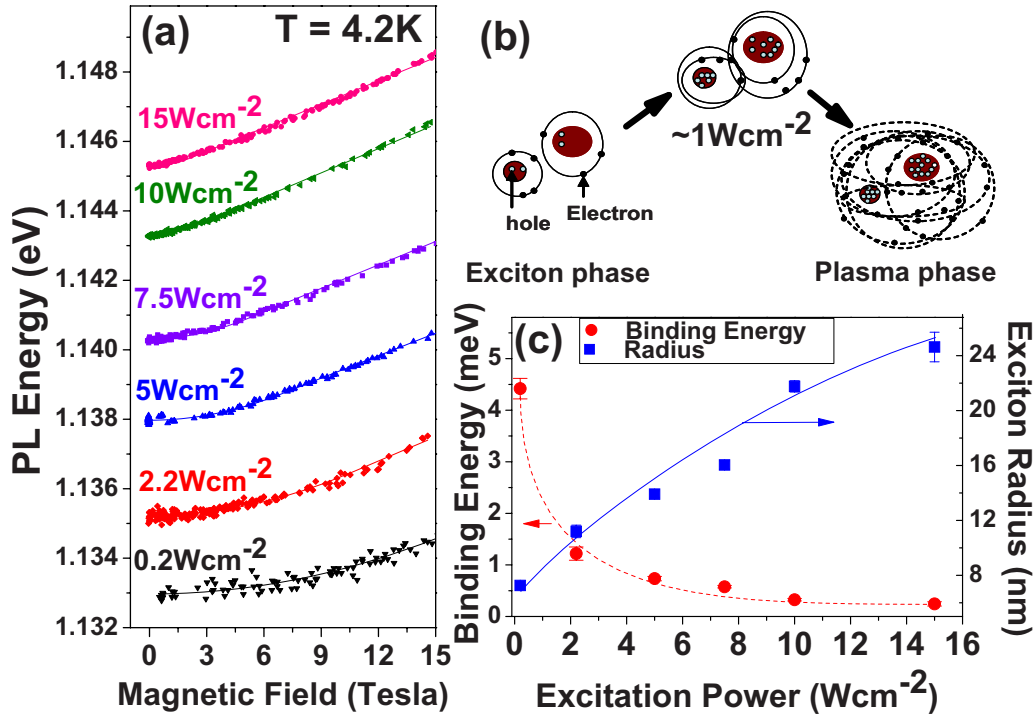


FIG. 3. (Color online) (a) PL peak transition energy as a function of magnetic field at different laser powers measured at 4.2 K. Solid lines are the fits to the equation $E_0 + \Delta E$, where ΔE is given by Eqs. (1) and E_0 is the zero-field transition energy that monotonically increases with excitation power. (b) A depiction of the corresponding electron trajectories (represented by solid lines for bound states and dotted lines for free particles) as the sample goes through a density-dependent Mott transition. (c) The values of the exciton radius (squares) and the exciton binding energy (circles) as a function of excitation power, obtained from the fits in (a). The smooth curves are just to guide the eye. The binding energy and the radius at 0.2 W cm⁻² excitation are obtained from fits to the data in Fig. 4(c) since a field of 15 T is not enough for excitons with radii ≤ 10 nm.

a weakly bimodal size distribution for the lateral diameters of the dots with the prominent mode at around 22 nm, subsequent cross-sectional scanning tunneling microscopy done with atomic scale resolution¹² revealed that the actual lateral extent of the dots is considerably smaller due to alloying and replacement of antimony by arsenic atoms. The dots had a lateral size of between 4–8 nm and were about 2 nm high.¹² The low temperature PL spectra exhibit two prominent peaks, from the wetting layer (WL) at about 900 nm and the QD ensemble at about 1100 nm (Fig. 2). The ratio of the WL to the QD PL intensities is strongly excitation power dependent. This gives an indication of the relative populations of carriers in the two regions. A U-shape of the PL peak energy as a function of excitation power was observed at ultralow excitation powers,¹¹ due to optically induced charge depletion of the unintentionally doped QDs. The present study is limited to higher powers where we observe the conventional blueshift [Fig. 3(a)], and the physics of charge depletion is not relevant. Note that the contribution of the capacitive charging energy associated with the increased hole occupancy at higher excitation powers^{7,10} completely masks the band gap renormalization effects.

PL measurements were performed in pulsed magnetic fields, $B \leq 48$ T, using a 532 nm excitation laser and an InGaAs diode array for detection. The magnetic field-induced shift of excitonic (hydrogenic) ground state at very low fields corresponds to a diamagnetic shift that is to the lowest order in perturbation theory quadratic in the magnetic

field, $\Delta E \sim [q^2 \langle \rho^2 \rangle / 8\mu] B^2$. The high field regime is equivalent to having “free” electrons and holes recombining from their respective Landau level ground states. Thus the shift is linear at very high fields, $\Delta E \sim [\hbar q / 2\mu] B$. q is the absolute value of the electron charge, μ the reduced mass of the electron-hole pair, and $\sqrt{\langle \rho^2 \rangle}$ is the exciton radius. These functional forms are strictly valid only in the two asymptotic limits, but are a good approximation¹³ for $\beta \leq 0.4$ and $\beta \geq 1$, respectively, if β is the ratio of the cyclotron energy to twice the effective exciton Rydberg energy. As the simplest approximation, a functional form for the magnetic field-dependent change in the peak position of the PL spectra (henceforth called PL peak shift) for $0.4 \leq \beta \leq 1.0$ may be extrapolated by demanding adiabatic continuity between the two regimes and assuming that diamagnetic contribution extends up to $\beta = 1$. This leads to the following phenomenologically successful relationship (e.g., Ref. 14) to describe the PL peak shift for all β :

$$\Delta E = \frac{q^2 \langle \rho^2 \rangle}{8\mu} B^2, \quad \text{for } B < B_c, \quad (1a)$$

$$\Delta E = -\frac{\hbar^2}{2\mu \langle \rho^2 \rangle} + \frac{\hbar q}{2\mu} B, \quad \text{for } B > B_c. \quad (1b)$$

The crossover field $B_c = 2\hbar / (q \langle \rho^2 \rangle)$. The first term in Eq. (1b) corresponds to the excitonic binding energy and is the ex-

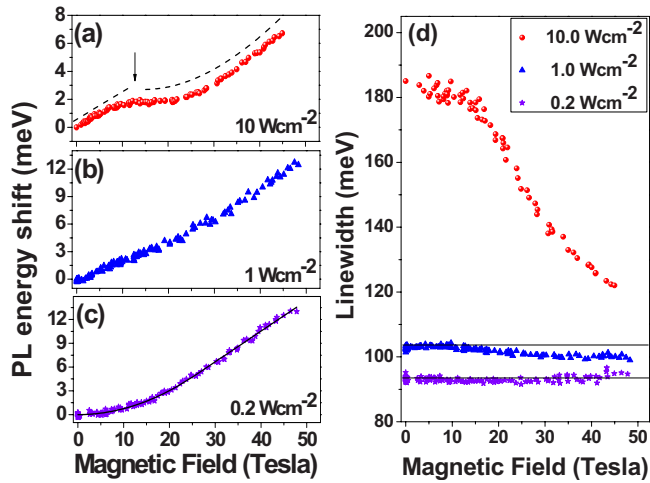


FIG. 4. (Color online) PL peak shift ($B \leq 48$ T) at different excitation powers. Cryostat temperature ~ 15 K. At high powers, (a) and (b), the slope of the PL peak shift shows an unexpected change at intermediate fields. At low power (c), the conventional excitonic behavior is observed and the PL peak shift is well described by Eq. (1) (solid line). (d) Magnetic field-dependent PL linewidths at different excitation powers. Solid lines are to guide the eye.

trapolation to $B=0$ of the high-field slope [second term in Eq. (1b)].

Figure 3(a) shows the PL peak shift (inferred from fitting the Gaussian line shape to the spectra) at different excitation powers measured in magnetic fields of up to about 15 T, with the sample at 4.2 K. Fitting these data to Eqs. (1) gives a direct way to measure the excitonic binding energies and the radii. The results are shown in Fig. 3(c). The value of the average binding energy of the exciton decreases from 4.5 meV to less than 0.5 meV as the excitation power is increased by one and a half orders of magnitude. The evolution is accompanied by the corresponding increase in the exciton radius from 8 nm to about 25 nm. We thus have an indication of the system progressing toward a Mott transition. The peak-shift observations correlate well with the zero-field emission spectra of Fig. 2, where despite the large inhomogeneous broadening, the loss of excitonic resonance is clearly observed by the broadening of the high energy tail and the significant increase in linewidth at high excitation power [also see Fig. 4(d)]. Reference 15 also reports a similar broadening.

The weakening of the binding of electrons from a specific site can be related to two effects. Of primary importance is the higher electron density, especially of those electrons which participate in the WL PL. Figure 2 shows that the WL PL intensity increases much faster than the QD PL intensity, implying a greater role of screening at higher excitation power. Specifically, there exists a critical screening length λ_c beyond which the positively charged dots do not support bound (exciton) states. While for a three-dimensional (3D) system with Yukawa interaction¹⁶ λ_c is $0.84a_B$, in the actual QD ensemble the barrier potentials at the QD-matrix hetero-interface further aid ionization. QDs are also not a homogeneous three-dimensional system because the electrons are constrained to the matrix above the dots (by the presence of

the WL), but still are attracted to the holes in the dots and the WL. Secondly, since the average separation of the *randomly located* QDs in the present sample is about 50–60 nm, for exciton sizes of about 25 nm there may be an overlap between some excitons with their neighbors. The delocalization of a few electrons can further aid in screening, leading to further ionization.

Figure 4 extends the study to much higher magnetic fields ($B < 48$ T). For practical reasons pertaining to helium turbulence during the pulse, the high field experiments had to be performed in a helium flow cryostat at a temperature of about 15 K. It is likely that the slight increase in temperature has further aided ionization. The observation of a very large linewidth in Fig. 2, at the excitation power of 10 W cm^{-2} , was indicative of the formation of the plasma phase. Now notice the anomaly in the PL peak shift of the spectra measured at this excitation power [Fig. 4(a)]. The PL peak shift shows an unexpected change in slope around 15 T and it can no longer be described by Eq. (1) in the entire field range. Qualitatively, a linear peak shift at low fields (indicative of the electron plasma state with near-zero binding energy [cf. Eq. (1)]) transforms to a curve described by Eq. (1) [dotted line in Fig. 4(a)]. This transition from linear to quadratic dependence is due to the magnetic field-induced stabilization⁴ of the insulating magnetoexciton state^{8,9}—an arbitrarily weak 1D (effective dimensionality is reduced on account of 2D magnetic confinement) potential must support at least one bound state. This is similar to the field-induced impurity freeze-out phenomenon⁴ of semiconductor physics. Between Figs. 4(a) and 4(b) (and other measurements at intermediate powers) we observe an increase in slope of the field dependence of the peak shift at low magnetic fields. This suggests a coexistence of two phases due to distribution of critical screening lengths for different sized QD in the ensemble. Note that Fig. 4(c), where we began with a clearly bound excitonic state at $B=0$, Eq. (1) [solid line in Fig. 4(c)] describes the PL peak shift in the entire field range and there is no Mott transition.

Independent evidence of the above described phenomena is provided by the difference in the field dependence of the linewidths of the spectra measured at different excitation powers [Fig. 2 (inset) and Fig. 4(d)]. The linewidth is nearly constant up to 45 T for the spectra measured at the excitation power of 0.2 and 1 W cm^{-2} , completely determined by the inhomogeneous broadening. Figure 2 (inset) shows that increasing the measurement temperature to as high as 185 K also does not affect the spectral shape.

On the other hand, there is $\sim 30\%$ decrease in the linewidth of the spectra measured at 10 W cm^{-2} [Fig. 4(d)] in an applied magnetic field. The linewidth is almost constant in plasma phase below 15 T and the decrease correlates with the anomaly in the peak-shift data. Furthermore, in high magnetic field, the linewidth again tends toward the inhomogeneous-broadening-limited value measured for the excitons at lower laser powers.¹⁷ Figure 4(d) thus serves the purpose of a rough “phase diagram,” where the upper part of the graph corresponding to large linewidths denotes the plasma phase and the lower part the (inhomogeneously broadened) exciton phase. Since the Mott transition is a zero-temperature phenomenon, the measurements described in

Fig. 4(d) and the rest of the paper only depict magnetic field-, excitation power-, and temperature-aided excursions to various phases.

The highly nonequilibrium nature of the phenomena requires the generation of a large number of photoexcited carriers and consequently sample excitation under high laser powers, resulting in some sample heating. However, this heating is only a perturbation to the experimental conditions: First, the zero-magnetic field PL spectra show a strong temperature dependence at all laser powers and they all merge to a single curve beyond 100 K (not shown). These observations indicate that the difference in the sample heating between the lowest and the highest powers is not more than a few kelvin. Furthermore, the loss of excitonic resonance due to many-body effects, which change the functional form of the spectral density, is different from the thermal ionization of excitons (Fig. 2). For the spectra measured at 185 K and the excitation power of 0.2 W cm^{-2} , the inhomogeneous linewidth is unaffected despite the large temperature change.

Finally, we mention that the emission intensities were magnetic field dependent. Unlike for type-I dots, we observed a magnetic field-induced PL quenching, which suggests that the ground state of magnetoexcitons in our sample is dark with a possibility of a gap that can be overcome at high temperatures.

We have studied the different phases of spatially indirect excitons in an ensemble of GaSb QDs contained within a GaAs matrix. We have observed systematic changes in the average excitonic binding energy and the Bohr radius with changing electron-hole density (Fig. 3). These are interpreted as the transition from an insulating excitonic phase to a single component plasma phase. The magnetic field-induced shift of the peak energy of the PL spectra, when the system is in the plasma phase, shows an anomalous functional form (Fig. 4) that is indicative of a phase transition. This is attributed to a second Mott transition back to the insulating magnetoexciton state. The loss and the recovery of the excitonic resonance has been independently tracked by observing the changes in the inhomogeneous linewidth as a function of excitation power and magnetic field [Fig. 2 and Fig. 4(d)].

This work is supported by the Belgian IAP, the SANDiE Network of Excellence (Contract No. NMP4-CT-2004-500101), and EuroMagNET (Contract No. RII3-CT-2004-506239) projects of the European Commission. BB acknowledges the support of FWO Vlaanderen and M.H. the Research Councils UK. We thank J. Vanacken and F. Herlach for their support and guidance in the pulsed-field experiments.

*Present address: IMM, High Field Magnet Laboratory HFML, University of Nijmegen, Toernooiveld 7, 6525 ED NIJMEGEN, The Netherlands; bhavtosh.bansal@science.ru.nl

¹R. Zimmermann, *Many-Particle Theory of Highly Excited Semiconductors* (Teubner, Leipzig, 1988).

²L. V. Butov, *J. Phys.: Condens. Matter* **16**, R1577 (2004).

³J. Shah, M. Combescot, and A. H. Dayem, *Phys. Rev. Lett.* **38**, 1497 (1977); G. Manzke, Q. Y. Peng, K. Henneberger, U. Neukirch, K. Hauke, K. Wundke, J. Gutowski, and D. Hommel, *ibid.* **80**, 4943 (1998); L. Kappei, J. Szczytko, F. Morier-Genoud, and B. Deveaud, *ibid.* **94**, 147403 (2005); A. Amo, M. D. Martin, L. Viña, A. I. Toropov, and K. S. Zhuravlev, *Phys. Rev. B* **73**, 035205 (2006).

⁴E. W. Fenton and R. R. Haering, *Phys. Rev.* **159**, 593 (1967).

⁵L. Müller-Kirsch, R. Heitz, U. W. Pohl, D. Bimberg, I. Hüsler, H. Kirmse, and W. Neumann, *Appl. Phys. Lett.* **79**, 1027 (2001).

⁶R. A. Hogg, K. Suzuki, K. Tachibana, L. Finger, K. Hirakawa, and Y. Arakawa, *Appl. Phys. Lett.* **72**, 2856 (1998); M. Geller, C. Kapteyn, L. Müller-Kirsch, R. Heitz, and D. Bimberg, *ibid.* **82**, 2706 (2003); E. R. Glaser, B. R. Bennet, B. V. Shanabrook, and R. Magno, *ibid.* **68**, 3614 (1996); F. Hatami, N. N. Ledentsov, M. Grundmann, J. Boehrer, F. Heinrichsdorff, M. Beer, D. Bimberg, S. S. Ruvimov, P. Werner, U. Goesele, J. Heydenreich, U. Richter, S. V. Ivanov, B. Ya. Meltser, P. S. Kop'ev, and Zh. I. Alferov, *ibid.* **67**, 656 (1995).

⁷M. Hayne, J. Maes, S. Bersier, V. V. Moshchalkov, A. Schliwa,

L. Müller-Kirsch, C. Kapteyn, R. Heitz, and D. Bimberg, *Appl. Phys. Lett.* **82**, 4355 (2003).

⁸K. L. Janssens, B. Partoens, and F. M. Peeters, *Phys. Rev. B* **64**, 155324 (2001).

⁹E. Ribeiro, A. O. Govorov, W. Carvalho, and G. Medeiros-Ribeiro, *Phys. Rev. Lett.* **92**, 126402 (2004); A. B. Kalametsev, V. M. Kovalev, and A. O. Govorov, *JETP Lett.* **68**, 669 (1998).

¹⁰K. Matsuda, S. V. Nair, H. E. Ruda, Y. Sugimoto, T. Saiki, and K. Yamaguchi, *Appl. Phys. Lett.* **90**, 013101 (2007).

¹¹M. Hayne, O. Razinkova, S. Bersier, R. Heitz, L. Müller-Kirsch, M. Geller, D. Bimberg, and V. V. Moshchalkov, *Phys. Rev. B* **70**, 081302(R) (2004).

¹²R. Timm, H. Eisele, A. Lenz, S. K. Becker, J. Grabowski, T.-Y. Kim, L. Müller-Kirsch, K. Pötschke, U. W. Pohl, D. Bimberg, and M. Dähne, *Appl. Phys. Lett.* **85**, 5890 (2004).

¹³R. P. Seisyan and B. P. Zakharchenya, in *Landau Level Spectroscopy*, Modern Problems in Condensed Matter Sciences Vol. 27.1 (North-Holland, Amsterdam, 1991), pp. 344–443.

¹⁴N. Schildermans, M. Hayne, V. V. Moshchalkov, A. Rastelli, and O. G. Schmidt, *Phys. Rev. B* **72**, 115312 (2005).

¹⁵L. Müller-Kirsch, R. Heitz, A. Schliwa, O. Stier, D. Bimberg, H. Kirmse, and W. Neumann, *Appl. Phys. Lett.* **78**, 1418 (2001).

¹⁶F. J. Rogers, H. C. Graboske, Jr., and D. J. Harwood, *Phys. Rev. A* **1**, 1577 (1970).

¹⁷This behavior (and the results in Fig. 3) cannot be explained by filling (Ref. 15) of discrete energy hole levels.